THE JOURNAL OF PHYSICAL CHEMISTRY B

ARTICLE

pubs.acs.org/JPCB

Phase Behavior of Rod−Coil Diblock Copolymer and Homopolymer Blends from Self-Consistent Field Theory

Wendi Song,[†] Ping Tang,[*,†] Feng Qiu,[†] Yuliang Yang,[†] and An-Chang Shi[†,‡]

[†]Key Laboratory of Molecular Engineering of Polymer, Ministry of Education, and Department of Macromolecular Science, Fudan University, Shanghai 200433, China

[‡]Department of Physics and Astronomy, McMaster University, Hamilton, L8S 4M1, Canada

ABSTRACT: The phase behavior of binary blends of rod−coil diblock copolymers and coil or rod homopolymers is studied by the self-consistent field theory (SCFT). The rod blocks are modeled as wormlike chains and the corresponding SCFT equations are solved using a hybrid method, in which the orientation-dependent functions are discretized on a unit sphere, while the positional space-dependent functions are treated using a spectral method. Phase diagrams of the blends are constructed as a function of the homopolymer volume fraction and phase segregation strength. It is discovered that the phase behavior of the system depends on the flexibility of the homopolymers. The addition of coil-homopolymers stabilizes the smectic phases. Low-molecular weight coil-homopolymers tend to mix with the coil-blocks, whereas high-molecular weight coil-homopolymers are mostly localized at the center of the coil-domains. On the other hand, the addition of rod-homopolymers strongly affects the orientation ordering of the system, leading to transitions between monolayer smectic-C, monolayer smectic-A and bilayer smectic-A phases.

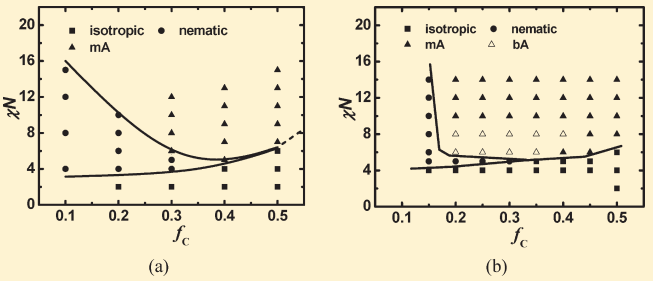

INTRODUCTION

Rod−coil block copolymers have attracted increasingly recent attention because they represent a unique polymeric system with potential applications to the manufacturing of various functional materials, including conjugated polymers as one of the most fascinating examples used in economic and efficient organic optoelectronic devices.[1−4] A desirable feature for these conjugated materials to be useful is their ability to self-assembly into well-defined nanostructures.[5,6] In contrast to coil−coil diblock copolymers, however, the phase behavior of rod−coil copolymers is significantly complex due to the anisotropic orientational interaction and chain rigidity of the rod-like blocks. The rigidity of these polymers originate from π-conjugation (semiconducting polymers), mesogenic unit, helical secondary structures (biomolecules), or aromatic groups (aramide and aromatic polyester high-performance resins).[7−12] Their self-assembly depends not only on the volume fraction of the coils, f_c, and the Flory−Huggins interaction between unlike blocks, χN, but also on other additional parameters, namely the liquid crystalline or orientational interaction between the rods, μN, the conformational asymmetry between the rods and coils, β, and the interplay between χN and μN. Previous experimental[13−16] and theoretical[17−23] studies have demonstrated complex phases including isotropic, nematic and smectic liquid crystal structures occurring in a wide range of coil fractions in the phase diagram, and interesting cylindrical structures with liquid crystal core or corona for side-chain liquid crystal block copolymers.[24−26] In particular, in contrast to coil−coil block copolymers, layered structures occupy a larger region of the phase space for rod−coil block copolymers due to the dominant orientational interaction between rods over the coils stretching entropy.

Furthermore, a domain size in the order of 10 nm is a crucial requirement for optoelectronic applications. One effective route to control the domain size in block copolymer systems is the addition of homopolymers which is chemically identical to one of the blocks. For rod−coil block copolymers, it has been demonstrated that adding homopolymers is an efficient method for controlling domain spacing, rod orientation, rod−coil interfacial property and transformation of various liquid crystalline phases without additional synthesis.[27−29] For coil−coil diblock copolymer and coil-homopolymer blends, the solubilization of the coil homopolymers have been studied extensively both experimentally and theoretically in the past few decades.[30−34] The mechanism of homopolymer solubilization depends primarily on the ratio of its molecular weight to that of diblock copolymers, which is similar to the case of wet or dry brush systems.[31] In contrast, for the case of the addition of rod-homopolymers, the solubilization is more complicated due to the anisotropic liquid crystalline interactions between the rod blocks, as well as the conformational asymmetry between the rods and coils. Recently Tao et al.[27] experimentally and theoretically investigated the domain size control of rod−coil

Received: March 1, 2011
Revised: June 2, 2011
Published: June 06, 2011

block copolymers by blending with molecular weight matched rod, coil, or rod and coil homopolymers. The lamellae period varies due to the different mechanisms of rod and coil homopolymer solubilization, which is in agreement with the self-consistent field theory (SCFT) and scaling theory. However, their SCFT simulations assumed completely rigid rod model and only focused on a monolayer smectic-A structure. Furthermore, a macrophase separation was predicted by SCFT at high homopolymer volume fractions, which was in discrepancy with the experimental results.

Therefore, systematical investigation of the effect of rod or coil homopolymers on the phase diagram and detailed microstructure including microdomain spacing, orientation of rods is highly desired. The SCFT based on the wormlike chain model for the rods[22,23,35] presents an accurate method to describe the phase behavior of polymers with some degree of chain rigidity. In this framework, the state of a polymer segment s is specified by its position $\mathbf{r}$ and its orientation $\mathbf{u}$, which represents two additional internal coordinates. In this case the numerical solution of the 6D diffusion equation including the angular Laplacian operator $\nabla_{\mathbf{u}}^2$ for the wormlike chain propagator $q(\mathbf{r},\mathbf{u},s)$, presents a computational challenge compared to that of Gaussian chain. Until now several numerical implementations have been proposed to solve the SCFT equations for wormlike chains, including spherical harmonic expansion[21,35] and real-space finite volume algorithm proposed by our group.[22] In the spherical harmonic method, the orientation-dependent functions are expanded by $Y_{l,m}(\mathbf{u})$ and the calculation is mostly restricted with axial-symmetry ($m = 0$) for simplicity. In contrast, the real-space method is a true 3D Euclidean space consideration of the orientational variables, which can distinguish smectic-C from smectic-A conveniently. In particular, our recent developed hybrid method[23] highly improved the solution accuracy and stability by a combination of real-space finite volume algorithm with the spectral method, where the space-dependent variables are expanded by a series of basis functions instead of the finite difference method in real-space.[22]

In this paper, we extend and apply the hybrid numerical SCFT approach to systematically examine the phase behavior of rod−coil block copolymers blended with coil or rod homopolymers. The stability of the layered structure in a larger region in the phase space allows it to persist even with the addition of large amounts of homopolymers. Therefore, we only focus on the lamellae structure and the controlling parameters in these blend systems include the Flory−Huggins interaction χN between the unlike rod and coil species, the Maier−Saupe interaction μN between the rigid rods, and the size asymmetry ratio between the rod and coil β. First the phase diagrams of rod−coil/coil and rod−coil/rod blends are constructed to explore the effects of additional homopolymers on the phase behavior. Second we examine the distribution of coil or rod homopolymers within the microstructure domains, to understand different solubilization mechanisms for rod and coil homopolymers. Finally, the SCFT results are compared with the experiments and scaling theory, to further understand the underlying physics of the blend phase behavior.

THEORETICAL MODEL AND NUMERICAL ALGORITHM

We consider an incompressible binary mixture of rod−coil diblock copolymers and coil or rod homopolymers confined in a volume V. Each diblock copolymer chain consists of N_{RC} monomers including N_{dC} coil segments and N_{dR} rod segments. Each coil homopolymer possesses N_{hC} segments, and each rod homopolymer possesses N_{hR} segments. The coil blocks and coil homopolymers are modeled as Gaussian chains characterized by a statistical segment length a, while the rod blocks and rod homopolymers are modeled as wormlike chains characterized by a statistical length b and a diameter d. For simplicity, the coil and rod segments are assumed to have the same monomeric volume, i.e., $a^3 = bd^2 = 1/\rho_0$, thus the coil volume fraction of the rod−coil diblocks is $f_{dC} = (N_{dC})/(N_{dC} + N_{dR}) = (N_{dC})/(N_{RC})$. Furthermore, the molecular weight of the coil homopolymers is characterized by the ratio between N_{hC} and N_{RC}, $\alpha = N_{hC}/N_{RC}$. For the rod homopolymers, we will consider the case with the same chain length as that of the rod blocks of the rod−coil block copolymers, $N_{hR} = N_{dR}$. The volume fractions of the added coil and rod homopolymers in the blends are denoted as f_{hC} and f_{hR}, thus the overall volume fractions of the coil components are $f_C = f_{hC} + (1 - f_{hC})f_{dC}$ in a rod−coil/coil blend and $f_C = (1 - f_{hR})f_{dC}$ in a rod−coil/rod blend, respectively. Similar to our previous papers,[23] a unit vector $\mathbf{u}(s)$ denotes the orientation of the s th rod segment and the geometrical asymmetry (topological disparity) between rods and coils is characterized by $\beta = bN_{RC}/a(N_{RC}/6)^{1/2}$. The SCFT study for the blend system is performed in a canonical ensemble, with a Flory−Huggins interaction χN describing the repulsion between the rods and coils, and a Maier−Saupe mean-field potential μN quantifying the anisotropic interactions between the rods. In the following expressions, all the spatial lengths are scaled by the unperturbed radius of gyration, $R_g = a(N_{RC}/6)^{1/2}$.

The hybrid method of numerically solving SCFT for rod−coil diblock melt is described in our previous paper in detail.[26] In this paper, we extend this method to blends of rod−coil diblock copolymers and coil or rod homopolymers. In the framework of the hybrid numerical method, only the spatial-dependence of a function is expanded in terms of basis functions, $g(\mathbf{r},\mathbf{u}) = \sum_j g_j(\mathbf{u})f_j(\mathbf{r})$.[36] For periodically ordered structures, the spatial-dependent basis functions $f_j(\mathbf{r})$ ($i = 1, 2, 3, ...$) are chosen as orthonormal eigenfunctions of the spatial Laplacian operator $\nabla_{\mathbf{r}}^2$ such that

$$\frac{1}{V}\int d\mathbf{r}\, f_i(\mathbf{r})f_j(\mathbf{r}) = \delta_{ij}, \quad \nabla_{\mathbf{r}}^2 f_i(\mathbf{r}) = -\lambda_i f_i(\mathbf{r}) \qquad (1)$$

In the current paper, we mainly focus on the lamellae (smectic) phases. Therefore, all spatial-dependent functions vary along with one dimension only, i.e., z-axis. The basis functions for this one-dimensional case can be chosen as follows:

$$f_i(z) = 1, \quad \sqrt{2}\cos\left(\frac{2\pi z}{D}\right), \quad \sqrt{2}\sin\left(\frac{2\pi z}{D}\right), \quad \sqrt{2}\cos\left(\frac{4\pi z}{D}\right), \quad \sqrt{2}\sin\left(\frac{4\pi z}{D}\right)... \qquad (2)$$

where D is the period of the ordered phases and z is the coordinate along the lamellae normal. The z-dependent end-segment distribution functions such as $q(z,s)$ and $q(z,\mathbf{u},s)$ can be expanded by $f_i(z)$. Thus, these functions are specified by the expansion coefficients, $q_{dC,i}(s)$, $q^{+}_{dC,i}(s)$ and $q_{dR,i}(\mathbf{u},s)$, $q^{+}_{dR,i}(\mathbf{u},s)$ for the coil and rod blocks, $q_{hC,i}(s)$ for the coil homopolymers and $q_{hR,i}(\mathbf{u},s)$, $q^{+}_{hR,i}(\mathbf{u},s)$ for the rod homopolymers, respectively.

The diffusion equation for $q_{dC,i}(s)$ and $q_{dR,i}(\mathbf{u},s)$ becomes:

$$\frac{\partial q_{dC,i}(s)}{\partial s} = -\lambda_i q_{dC,i}(s) - \sum_j \sum_k \Gamma_{ijk} q_{dC,j}(s) w_{C,k} \quad (0 \le s \le f_{dC}) \tag{3}$$

with the initial condition of $q_{dC,i}(0) = \delta_{i1}$. Similarly, the differential equation determining the propagator of the rod-like blocks is given by

$$\frac{\partial q_{dR,i}(\mathbf{u},s)}{\partial s} = -\beta \mathbf{u} \sum_j A_{ij} q_{dR,j}(\mathbf{u},s) + \frac{1}{2\kappa}\nabla_{\mathbf{u}}^2 q_{dR,i}(\mathbf{u},s)$$
$$- \sum_j \sum_k \Gamma_{ijk}\left[w_{R,k} - \mathbf{M}_k : \left(\mathbf{uu} - \frac{\mathbf{I}}{3}\right)\right] q_{dR,j}(\mathbf{u},s) \quad (f_{dC} \le s \le 1) \tag{4}$$

with the initial condition of $q_{dR,i}(\mathbf{u},f_{dC}) = q_{dC,i}(f_{dC})$. Because the two ends of the rod−coil diblocks are distinct, two conjugate propagator coefficients are required to complete the description of the diblock chain conformations.

$$\frac{\partial q^+_{dR,i}(\mathbf{u},s)}{\partial s} = -\beta \mathbf{u} \sum_j A_{ij} q^+_{dR,j}(\mathbf{u},s) - \frac{1}{2\kappa}\nabla_{\mathbf{u}}^2 q^+_{dR,i}(\mathbf{u},s)$$
$$+ \sum_j \sum_k \Gamma_{ijk}\left[w_{R,k} - \mathbf{M}_k : \left(\mathbf{uu} - \frac{\mathbf{I}}{3}\right)\right] q^+_{dR,j}(\mathbf{u},s) \quad (f_{dC} \le s \le 1) \tag{5}$$

with the initial condition of $q^+_{dR,i}(\mathbf{u},1) = \delta_{i1}$.

$$\frac{\partial q^+_{dC,i}(s)}{\partial s} = \lambda_i q^+_{dC,i}(s) + \sum_j \sum_k \Gamma_{ijk} q^+_{dC,j}(s) w_{C,k} \quad (0 \le s \le f_{dC}) \tag{6}$$

with the initial condition of $q^+_{dC,i}(f_{dC}) = (1)/(4\pi)\int d\mathbf{u} q^+_{dR,i}(\mathbf{u}, f_{dC})$. The coil homopolymer chain conformation can be simply described by the one chain propagator coefficient as,

$$\frac{\partial q_{hC,i}(s)}{\partial s} = -\lambda_i q_{hC,i}(s) - \sum_j \sum_k \Gamma_{ijk} q_{hC,j}(s) w_{C,k} \quad (0 \le s \le \alpha) \tag{7}$$

with the initial condition of $q_{hC,i}(0) = \delta_{i1}$. Similarly, the rod homopolymer chain propagators can be simply described by a pair of propagator coefficients $q_{hR,i}(\mathbf{u},s)$ and $q^+_{hR,i}(\mathbf{u},s)$ as in eqs 4 and 5, where $0 \le s \le 1 - f_{dC}$. But the initial conditions are $q_{hR,i}(\mathbf{u},0) = \delta_{i1}$ and $q^+_{hR,i}(\mathbf{u},1 - f_{dC}) = \delta_{i1}$. In the above expressions, the structure of the system is characterized by the eigenvalues and overlap integrals of the eigenfucntions, which are defined by,

$$\lambda_i = \begin{cases} 0 & \text{if } i = 1 \\ \left(\frac{i\pi}{D}\right)^2 & \text{if } i \text{ even} \\ \left(\frac{(i-1)\pi}{D}\right)^2 & \text{if } i \text{ odd} \end{cases} \tag{8}$$

$$A_{ij} = \frac{1}{D}\int \mathrm{d}z\, f_i(z)\nabla f_j(z) \tag{9}$$

$$\Gamma_{ijk} = \frac{1}{D}\int \mathrm{d}z\, f_i(z) f_j(z) f_k(z) \tag{10}$$

where Γ_{ijk} is a symmetric tensor, and A_{ij} is an antisymmetric matrix. The parameter κ in eqs 4 and 5 represents the bending rigidity, which is nondimensionalized by N_{RC}. Similar to our previous studies, we will set as $\kappa = 30$ to model rigid rods. The single chain partition functions for rod−coil diblocks, coil homopolymers and rod homopolymers are given, respectively, by

$$Q_{RC} = \frac{1}{4\pi}\int \mathrm{d}\mathbf{u}\, q_{dR,1}(\mathbf{u},1), Q_{hC} = q_{hC,1}(\alpha),$$
$$Q_{hR} = \frac{1}{4\pi}\int \mathrm{d}\mathbf{u}\, q_{hR,1}(\mathbf{u},1 - f_{dC}) \tag{11}$$

The coefficients of density distributions for coil blocks $\varphi_{dC,i}$ and rod blocks $\varphi_{dR,i}$ are given by:

$$\varphi_{dC,i} = \frac{f_{RC}}{Q_{RC}}\int_0^{f_{dC}} \mathrm{d}s \sum_j \sum_k q_{dC,j}(s) q^+_{dC,k}(s)\Gamma_{ijk} \tag{12}$$

$$\varphi_{dR,i} = \frac{f_{RC}}{4\pi Q_{RC}}\int_{f_{dC}}^1 \mathrm{d}s \int \mathrm{d}\mathbf{u} \sum_j \sum_k q_{dR,j}(\mathbf{u},s) q^+_{dR,k}(\mathbf{u},s)\Gamma_{ijk} \tag{13}$$

where f_{RC} is the average volume fraction of rod−coil diblock copolymers, with $f_{RC} = 1 - f_{hC}$ and $f_{RC} = 1 - f_{hR}$ in the rod−coil/coil and rod−coil/rod blend systems, respectively. The coefficients of density distributions for coil homopolymers $\varphi_{hC,i}$ and rod homopolymers $\varphi_{hR,i}$ are

$$\varphi_{hC,i} = \frac{f_{hC}}{Q_{hC}}\int_0^{\alpha} \mathrm{d}s \sum_j \sum_k q_{hC,j}(s) q_{hC,k}(\alpha - s)\Gamma_{ijk} \tag{14}$$

$$\varphi_{hR,i} = \frac{f_{hR}}{Q_{hR}}\int_0^{1-f_{dC}} \mathrm{d}s \int \mathrm{d}\mathbf{u} \sum_j \sum_k q_{hR,j}(\mathbf{u},s) q^+_{hR,k}(\mathbf{u},s)\Gamma_{ijk} \tag{15}$$

The amplitudes of potential fields acted on the coil and rod components are

$$w_{C,i} = \chi N(\varphi_{dR,i} + \varphi_{hR,i} - \delta_{i1}(1 - f_C)) + \xi_i \tag{16}$$

$$w_{R,i} = \chi N(\varphi_{dC,i} + \varphi_{hC,i} - \delta_{i1} f_C) + \xi_i \tag{17}$$

The orientational parameter and Maier−Saupe potential field are

$$\mathbf{S}_i = \frac{1}{4\pi Q_{RC}}\int_{f_{dC}}^1 \mathrm{d}s \int \mathrm{d}\mathbf{u} \sum_j \sum_k q_{dR,j}(\mathbf{u},s) q^+_{dR,k}(\mathbf{u},s)\left(\mathbf{uu} - \frac{\mathbf{I}}{3}\right)\Gamma_{ijk}$$
$$+ \frac{1}{4\pi Q_{hR}}\int_0^{1-f_{dC}} \mathrm{d}s \int \mathrm{d}\mathbf{u} \sum_j \sum_k q_{hR,j}(\mathbf{u},s) q^+_{hR,k}(\mathbf{u},s)\left(\mathbf{uu} - \frac{\mathbf{I}}{3}\right)\Gamma_{ijk} \tag{18}$$

The second term of the right side of eq 18 disappears in the rod−coil/coil blends. Furthermore, we define,

$$\mathbf{M}_i = \mu N \mathbf{S}_i \tag{19}$$

The system is subjected to the incompressibility condition

$$\varphi_{dR,i} + \varphi_{dC,i} + \varphi_{hC,i} + \varphi_{hR,i} = \delta_{i1} \tag{20}$$

where ξ_i in eq 20 is chosen to be $\xi_i = \lambda(\varphi_{dR,i} + \varphi_{dC,i} + \varphi_{hC,i} + \varphi_{hR,i} - \delta_{i1}$, where λ should be large enough to enforce the incompressibility of the system. Once the self-consistent field equations, i.e., the above amplitudes are numerically solved, the

real-space representations for the density distributions can be calculated as:

$$\varphi_{dC}(z) = \sum_i \varphi_{dC,i} f_i(z), \varphi_{dR}(z) = \sum_i \varphi_{dR,i} f_i(z) \quad (21)$$

The expressions for $\varphi_{hC}(z)$, $\varphi_{hR}(z)$, $w_C(z)$, $w_R(z)$, $\mathbf{S}(z)$, $\mathbf{M}(z)$ and $\xi(z)$ are analogous. Within the SCFT framework, the Helmholtz free energy of the rod−coil/coil blends is given by:

$$\frac{F_{(1)}}{nk_BT} = \frac{1}{V}\int d\mathbf{r}\left[\chi N(\varphi_{dC}+\varphi_{hC})\varphi_{dR} - w_C(\varphi_{dC}+\varphi_{hC}) - w_R\varphi_{dR} - \xi(1-\varphi_{dC}-\varphi_{dR}-\varphi_{hC}) + \frac{1}{2}\mathbf{M}:\mathbf{S}\right] - (1-f_{hC})\ln\frac{Q_{RC}}{(1-f_{hC})} - \frac{f_{hC}}{\alpha}\ln\frac{\alpha}{f_{hC}}Q_{hC} \quad (22)$$

and the Helmholtz free energy of the rod−coil/rod blends is given by:

$$\frac{F_{(2)}}{nk_BT} = \frac{1}{V}\int d\mathbf{r}\left[\chi N\varphi_{dC}(\varphi_{dR}+\varphi_{hR}) - w_C\varphi_{dC} - w_R(\varphi_{dR}+\varphi_{hR}) - \xi(1-\varphi_{dC}-\varphi_{dR}-\varphi_{hR}) + \frac{1}{2}\mathbf{M}:\mathbf{S}\right] - (1-f_{hR})\ln\frac{Q_{RC}}{(1-f_{hR})} - \frac{f_{hR}}{1-f_{dC}}\ln\frac{(1-f_{dC})}{f_{hR}}Q_{hR} \quad (23)$$

For the calculation of the SCFT equations composed of the expansion coefficients, the potential and orientational fields are updated using eqs 16−19 by means of a linear mixing of new and old solutions. These steps are repeated until self-consistency is achieved. During each step, the key and time-consuming procedure is the solution of propagator coefficients in diffusion-like eqs 4 and 5. The angular Laplacian such as $\nabla_{\mathbf{u}}^2 q_{dR,i}(\mathbf{u},s)$ is calculated by the finite volume algorithm with the orientation variable $\mathbf{u}$ discretized on the surface of a unit sphere like our previous work.[23] In order to ensure that the convergence of free energy, the number of basis functions is set in the N_i = 13−31 range for different interaction conditions. N_s = 800 contour points are used to resolve the s dependence, to ensure the discretization of $\Delta s = 1/N_s$ sufficient to obtain accuracy of the order of 10^{-6} in the potential fields (including compositional and orientational potentials). The solution for a certain period length D and tilt angle θ is proven to rapidly achieve self-consistence with the free energy accuracy in the order of 10^{-4}. Finally the equilibrium morphology is obtained according to the minimization of free energy iterated with respect to variety of reasonable simulation box sizes and different initial guess of the orientational direction.

RESULTS AND DISCUSSION

Recently, as the first application of the hybrid numerical SCFT method, we have constructed phase diagrams of rod−coil diblock copolymers as a function of the ratio between orientational interaction and microphase separation, i.e., the ratio μ/χ, and the topological disparity between the rod and coil blocks β.[23] It was demonstrated that the stability of various smectic phases depends strongly on μ/χ and β. In the current study, we choose a compositionally symmetric rod−coil diblock copolymer (f_{dC} = 0.5), which self-assembles into monolayer smectic-A phase (mA) at μ/χ = 4 and β = 4 for χN above the order−disorder transition (ODT), to examine the influence of the added homopolymers on the phase behavior. Three different coil homopolymers, characterized by a ratio of the molecular weight of coil homopolymers to rod−coil copolymers such as α = 1/8, 1/2 and 1, and molecular weight matched rod homopolymers ($N_{hR} = N_{dR}$) are chosen to be blended with the rod−coil block copolymers.

A. Rod−Coil/Coil Blends. *Phase Diagrams.* We first present the phase diagram in the plane defined by χN (with a fixed μ/χ = 4) and the overall volume fraction of coils f_C for various values of α, i.e., different molecular weights of homopolymers (Figure 1). To make a straightforward comparison, the phase diagram of pure rod−coil diblock copolymers is shown as Figure 1a, which was obtained in our recent paper.[23] In this section we restrict our attention to the χN-values extending from the ODT between the isotropic and smectic phases to intermediate segregation area (χN = 6−14).

A common feature emerging from Figure 1 is that the area of the ordered smectic structures is enlarged with the addition of the coil homopolymers. This result is in agreement with the experimental observations of unusual stability of lamellae in rod−coil/coil blends with large amounts of molecular weight matched homopolymers incorporated.[27] In particular, the results show that even the low molecular weight coil homopolymers, such as the case of α = 1/8, have the ability to stabilize the ordered smectic phases of rod−coil diblock copolymers, as evidenced by a comparison between Figure 1a and 1b. This behavior is quite different from the case of coil−coil AB diblock copolymer and coil A homopolymer blend system, where the low molecular weight homopolymer such as α < 1/4 is predicted to disorder a microstructure because of the entropy gain due to a uniform homopolymer distribution throughout the blends.[31] This difference can be understood by the orientational interaction between rod blocks. The orientational interaction drives the rods to be aligned to one preferred direction, i.e., the nematic director $\mathbf{n}$, leading to a fine smectic monolayer of rods, thus preventing the coil penetration into the rod-domains. Another feature from Figure 1 is that the region of smectic phases expands significantly with the increase of the molecular weight of coil homopolymers (α), from Figure 1b to Figure 1d, resulting in a larger critical volume fraction of coils f_C for the isotropic−smectic transition in the phase diagram. However, the three different molecular weight coil homopolymers exhibit different solubilization mechanisms into the matrix of diblock copolymer lamellae, which will be discussed in detail in the following section.

The series of rod−coil/coil blends also present a critical value of χN for the ODT similar to the case of AB/A coil blends.[31] When the system is below χN = 6, or the ODT of the pure rod−coil diblocks, the coil homopolymers are completely miscible with the diblocks and only an isotropic state is found. Therefore, the addition of coil homopolymers hardly changes the ODT at f_C = 0.5 of pure rod−coil diblock copolymers. Moreover, the three rod−coil/coil blends examined here do not undergo macrophase separation, which however occurred at the AB/A coil blends with the addition of high molecular weight homopolymers.[31]

It is noted that the monolayer smectic-C (mC) phase observed in the neat rod−coil diblocks at χN = 12 in Figure 1a disappears and the mA occurs instead when blended with coil homopolymers in Figure 1, parts b−d. The stabilization of the mA results from the solubilization of homopolymers, which can relax the stretching entropy of coil blocks. With the increasing of the molecular weight of the coil homopolymers (α), this

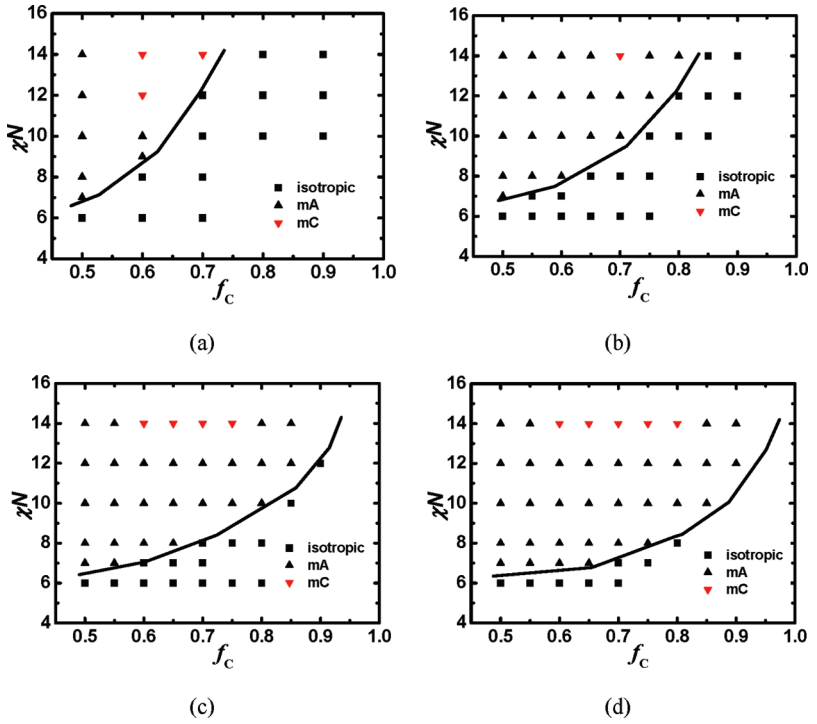

Figure 1. Phase diagrams for a symmetric rod−coil diblock (f_{dC} = 0.5) blended with different molecular weight (denoted by the ratio α) coil homopolymers as a function of χN and f_C with $\mu/\chi = 4$ and $\beta = 4$. Solid lines are guide to the eye denoting phase boundaries between the isotropic and smectic phases. Key: (a) the pure rod−coil diblocks; (b) α = 1/8; (c) α = 1/2; (d) α = 1.

solubilization effect becomes weaker and thus the stability of the mC instead of mA at χN = 14 significantly increases. According to the polymer brush theory, when the coil homopolymer is shorter than the coil block such as α = 1/8, the short homopolymers can penetrate into the coil blocks to form the so-called wet brush. Then the rod blocks are laterally pushed apart, creating more space for the chain relaxation of coil blocks, thus favoring the mA in Figure 1b. When the coil homopolymers are the same (α = 1/2) length or longer (α = 1) than the coil blocks, the distance of their penetration into the coil blocks decreases to form so-called dry brush, where the long homopolymers are pushed toward the center of coil-rich area. In this case, the rod blocks need to tilt an angle to the lamellae normal (formation of the mC) to release the coil stretching entropy penalty.

Microstructure and Lamellae Period. The various effects such as the molecular weight α and volume fraction f_{hC} of added homopolymers on the microstructure of smectic phases and lamellae period are examined in this section. To be specific, we consider the slices through the phase diagrams at a certain χN. Taking advantage of numerical SCFT, various detailed distribution profiles can be obtained, including the densities for coil homopolymers $\varphi_{hC}(z)$, coil blocks $\varphi_{dC}(z)$ and rod blocks $\varphi_{dR}(z)$, as well as the rod block terminals $\varphi_{dR}(z,s = 1)$ and the rod−coil junctions $\varphi_{dR}(z,s = f_{dC})$ according to the definition in ref 23.

Figure 2 shows the detailed density distributions for two representative rod−coil/coil blends, i.e., f_{hC} = 0.2 and f_{hC} = 0.5, corresponding to f_C = 0.6 and f_C = 0.75. When χN = 12, the pure rod−coil diblock copolymers will adopt mC for f_C = 0.6 and isotropic for f_C = 0.75 according to Figure 1a. However, from Figure 2, the mA is observed in the blends both for low molecular weight coil homopolymer α = 1/8 and relatively high molecular weight coil homopolymer α = 1. For α = 1/8, the small molecular weight coil homopolymers mainly distribute throughout the coil-rich area and mix well with the coil blocks, only small quantity of homopolymers penetrating into the rod domain at high homopolymer loadings, i.e., f_{hC} = 0.5 (f_C = 0.75), as shown in Figure 2a. The rod−coil interfacial area increases due to the swelling of short coil homopolymers, which can provide more space to release the stretching entropy penalty of coil blocks. Therefore, two increasing density peaks of $\varphi_{dC}(z)$ near the rod−coil interface are found in Figure 2a, at the cost of high interfacial energy. This evolution of coil block density distribution is also observed in the system of α = 1 in Figure 2b. However, like dry polymer brushes, the high molecular weight coil homopolymers are completely prevented from penetrating into the interfacial region and distribute at the center of coil-rich area even at low loadings, i.e., f_{hC} = 0.2 (f_C = 0.6). A significant sublayer of homopolymers where $\varphi_{hC}(z)$ approaches 1 is observed when f_{hC} is increased to 0.5 (f_C = 0.75), as shown in Figure 2b. This induces a continuous unbinding transition for the coil blocks, where $\varphi_{dC}(z)$ approaches 0 at the center of coil domain area, similar to the expectation in the traditional AB/A coil blends.[31]

Comparing the rod block densities between parts a and b of Figure 2, the case of α = 1/8 experiences a slight decrease in the density profile $\varphi_{dR}(z)$ as f_{hC} increases from 0.2 to 0.5, while the completely unchanged distribution $\varphi_{dR}(z)$ is found for the system of α = 1. In particular, the specific segment distributions, $\varphi_{dR}(z,s = 1)$ and $\varphi_{dR}(z,s = f_{dC})$ in Figure 2c and 2d, both exhibit two-peak distribution near the rod−coil interface, suggesting the unchanged interdigitate monolayer structure in the rod domain both for α = 1/8 and α = 1. Moreover the orientation degree $S_{zz}(z)$, which is the *zz* component of the orientational tensor $\mathbf{S}(z)$ as defined in ref 23, persists at a high level and even approaches 1 in the rod sublayers for a large quantity of coil homopolymer

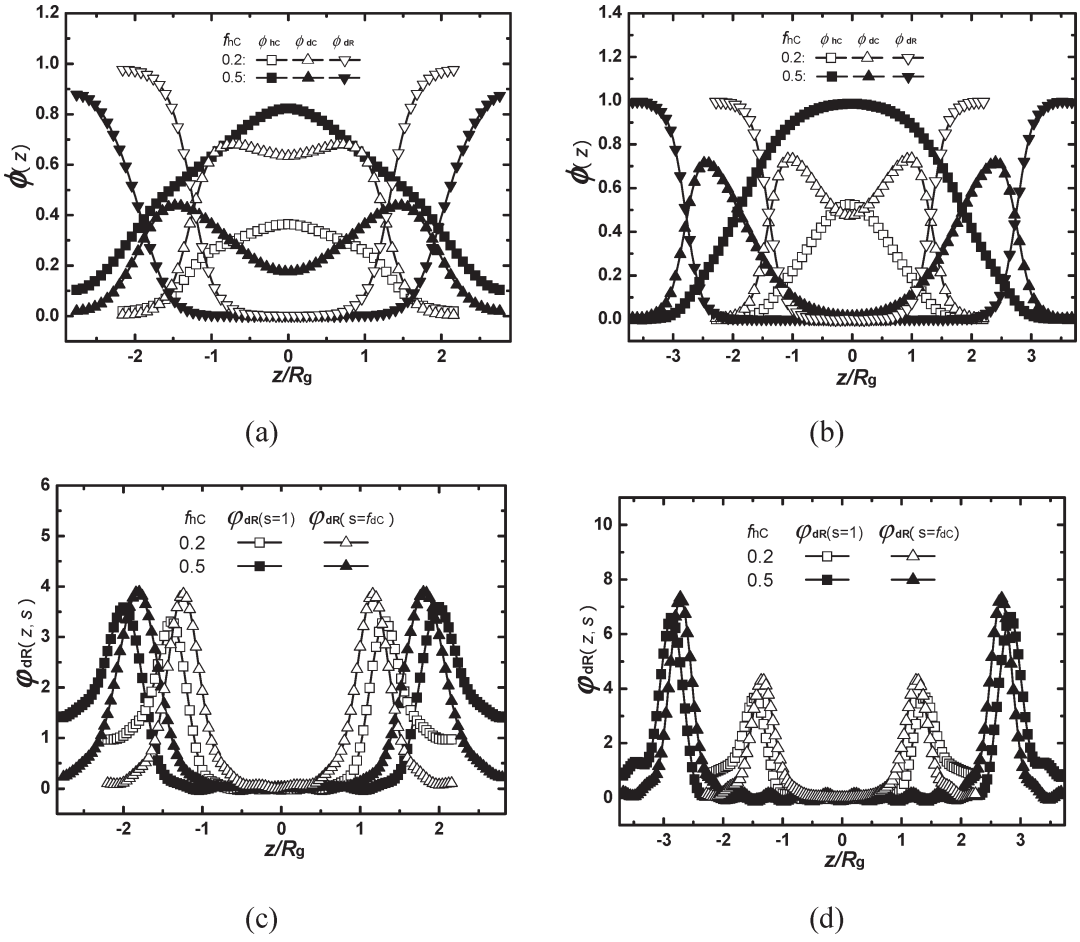

Figure 2. Density distributions of coil homopolymers $\varphi_{hC}(z)$, coil blocks $\varphi_{dC}(z)$ and rod blocks $\varphi_{dR}(z)$ at $f_{hC} = 0.2$ and $f_{hC} = 0.5$, as a function of z, with $z = 0$ located at the center of coil-rich area for (a) $\alpha = 1/8$ and (b) $\alpha = 1$. The density distribution of rod terminals $\varphi_{dR}(z,s = 1)$ and rod−coil junctions $\varphi_{dR}(z,s = f_{dC})$ for (c) $\alpha = 1/8$ and (d) $\alpha = 1$.

additions (figures not shown here). This phenomenon is in agreement with the observation of experimental results,[27] where the wide-angle X-ray scattering (WAXS) profiles indicated no perceptible changes in the rod domain size and rod−rod spacing. This is reasonable because the liquid crystalline characteristic of rods can preserve its microstructure better than that of flexible blocks. Furthermore, the anisotropic interaction between rods and less entropy loss of rods at the rod−coil interface both favor the flat interface and further maintain the stability of liquid crystalline structure in the self-assembly of rod−coil block copolymer system.

To better understand the effect of the addition of coil homopolymers on the blend phase behavior, we examine the domain sizes including the coil homopolymer rich area D_{hC}, the overall coil-rich area D_C, rod-rich area D_R and the overall lamellae period D, as well as the homopolymer and diblock copolymer interfacial width w_{hd}, and the rod−coil interfacial width w_{RC}, where all the lengths are in units of R_g. In this calculation, we define that the interface between homopolymers and rod−coil diblock copolymers as the inflection points $z = z_0$ where the second derivative of $\varphi_{hC}(z_0)$ is zero, and thus the interfacial width is given by $w_{hd} = |(d)/(dz)\varphi_{hC}(z)|_{z=z_0}{}^{-1}$. Similarly, the interface between rods and coils is given by $w_{RC} = |(d)/(dz)\varphi_C(z)|_{z=z'_0}{}^{-1}$, with $z = z'_0$ pointing to the location for the zero value of second derivative of $\varphi_C(z)$. The numerical SCFT results at $\chi N = 12$ for different values of α are shown in Figure 3.

Parts a and b of Figure 3 show the domain size D_{hC}, D_C, D_R as well as w_{hd} for low molecular weight homopolymer $\alpha = 1/8$ and high molecular weight one $\alpha = 1$. For the case of $\alpha = 1/8$ in Figure 3a, D_{hC} is approximately equals to D_C, suggesting that the coil homopolymers are well dissolved in the coil-block area, which in turn decreases the stretching entropy penalty of coil blocks. This result can be attested by the density profiles, $\varphi_{hC}(z)$ and $\varphi_{dC}(z)$ in Figure 2a. However for $\alpha = 1$, a large difference between D_{hC} and D_C is observed. From the density profiles in Figure 2b, high molecular weight homopolymers are expelled from the coil blocks like the case of dry brush, and the interfacial width w_{hd} between the homopolymers and diblock copolymers is much smaller than that for $\alpha = 1/8$. The results indicate that the solubilization between coil homopolymers and coil blocks decreases as the increasing of α, which is in agreement with the prediction of AB/A coil blends[31] and polymer brush theory. The resultant dependency of D and w_{RC} on α can be revealed in Figure 3c and 3d, the addition of low molecular weight homopolymers ($\alpha = 1/8$ and $\alpha = 1/2$) increases the overall lamellae period D and D_C slowly, but the high molecular weight homopolymer ($\alpha = 1$) increases D (D_C) much quickly with enhancing f_{hC}. Unlike the AB/A coil blends, however, the solubilization of coil homopolymers hardly influences the liquid crystalline structure of rod blocks. Figure 3a and 3b show the unchanged rod domain size D_R with the increase of added coil homopolymers

dx.doi.org/10.1021/jp201972n |J. Phys. Chem. B 2011, 115, 8390–8400

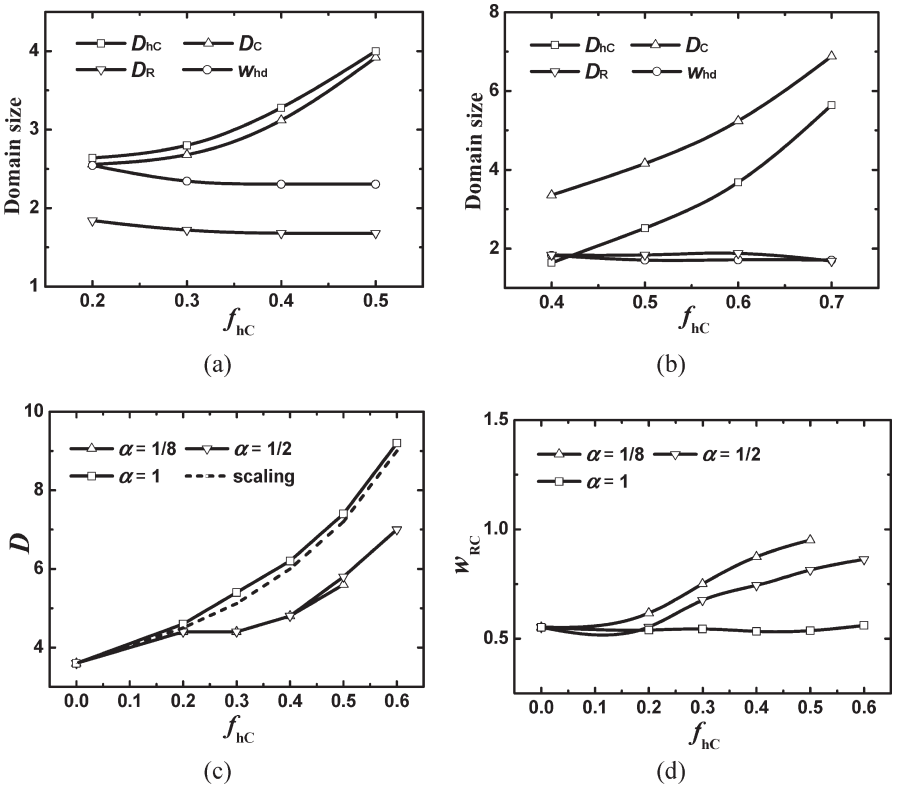

Figure 3. The domain sizes for coil homopolymers D_{hC}, the overall coils D_C and rods D_R as well as the homopolymer-diblock copolymer interfacial width w_{hd} as a function of f_{hC} under $\chi N = 12$ for (a) $\alpha = 1/8$ and (b) $\alpha = 1$. The lamellae period D and rod−coil interfacial width w_{RC} are shown in (c) and (d) respectively for three different molecular weight values of α with SCFT calculations. The dashed line in part c denotes the scaling theory result, consistent with SCFT for $\alpha = 1$.

for both $\alpha = 1/8$ and $\alpha = 1$. Moreover, the rod domain size D_R is the same between $\alpha = 1/8$ and $\alpha = 1$.

In addition, we calculate the swollen lamellae spacing of rod−coil/coil blends using a scaling theory in strong segregation limit, with the assumption of a simple volumetric approach as performed in ref 27. In the framework of scaling theory, the lamellae period is defined as $D' = (D_0)/(1 - f_{hC})$, where D_0 is the period length of pure rod−coil diblocks. The plot of D' is inserted to Figure 3c, which shows a good agreement with our SCFT result for $\alpha = 1$. But small molecular weight homopolymers ($\alpha = 1/8$ and $\alpha = 1/2$) exhibit considerable departure from the scaling theory. This discrepancy can be understood by examining the rod−coil interfacial width w_{RC} in Figure 3d. The interfacial width w_{RC} between rods and coils increases with the addition of coil homopolymers f_{hC} for low molecular weight case such as $\alpha = 1/8$ and $\alpha = 1/2$, while w_{RC} remains unchanged for $\alpha = 1$, due to different solubilization mechanisms for different molecular weight homopolymers as mentioned above. Therefore, the scaling theory based on the strong segregation assumption is applicable for examining the solubilization of added homopolymers with high enough molecular weight. This is the reason for the departure between experimental results and scaling theory in ref 27, where the added homopolymers with a moderate molecular weight predicted a slower increase of domain spacing than the scaling theory.

In conclusion, the addition of coil homopolymers can increase the stability of ordered smectic phases of rod−coil block copolymers. The effect of molecular weight of coil homopolymers plays a similar role in the microstructure of coil blocks to that in AB/A coil blends, similar to the case of polymer brush. However, the microstructure and orientation of the rod blocks are almost unchanged with the addition of the coil homopolymers due to their dominant chain rigidity and mutual orientational interactions. In particular, the coil domain size D_C and lamellae period D increase slower with the addition of small molecular weight coil homopolymers ($\alpha = 1/8, 1/2$) than the case of high molecular weight ($\alpha = 1$). These results provide a good strategy for performance optimization by blending suitable molecular weight coil homopolymers, to modify the microstructure but preserve the liquid crystalline feature in organic optoelectronic device based on the rod−coil self-assembly.

B. Rod−Coil/Rod Blends. *Phase Diagrams.* We first present the phase diagram of rod−coil/rod blends as a function of χN (μN) and f_C. Similar to the addition of coil homopolymers, a symmetric rod−coil diblock copolymer ($f_{dC} = 0.5$) is blended with a molecular weight matched rod homopolymer ($N_{hR} = N_{dR}$). The interactional condition is still assumed in the range from weak to intermediate segregation area ($\chi N = 4-14$). As shown in Figure 4, there are two main changes in the phase diagram of rod−coil/rod blends in Figure 4b compared to that of pure rod−coil diblocks in Figure 4a. First, a large portion of the nematic phase is replaced with the ordered smectic phases with the addition of the rod homopolymers at $f_{hR} = 0.4-0.6$ ($f_C = 0.2-0.3$). This increased stability of the ordered smectic phases is similar to that of the rod−coil/coil blends studied in section A. While Tao et al.[27] predicted the macrophase separation of rod−coil/rod blends at high volume fraction of rod homopolymers, i.e., $f_{hR} > 0.2$ based on the SCFT in the limit of completely rigid rod chains.

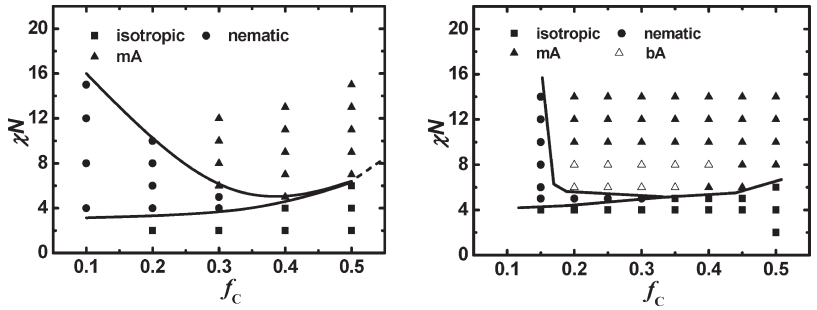

Figure 4. Phase diagrams for a symmetric rod−coil diblock ($f_{dC} = 0.5$) blended with molecular weight matched rod homopolymers as a function of χN and f_C at $\mu/\chi = 4$ and $\beta = 4$. Solid lines are guide to the eye denoting phase boundaries between isotropic, nematic and smectic phases. (a) pure rod−coil diblocks and (b) rod−coil/rod blends.

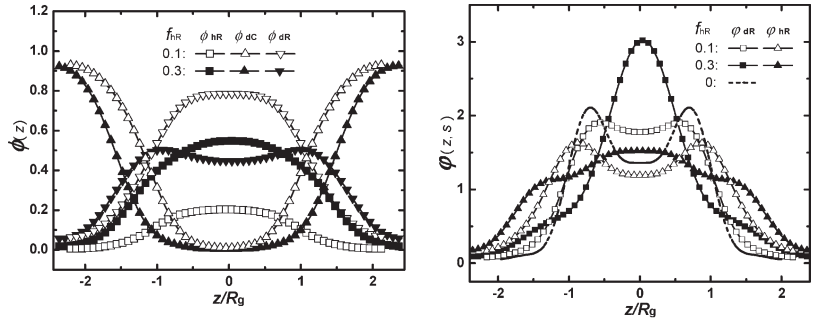

Figure 5. Density distributions of rod homopolymers $\varphi_{hR}(z)$, coil blocks $\varphi_{dC}(z)$ and rod blocks $\varphi_{dR}(z)$ as a function of z at $\chi N = 8$ in part a, and the plots of rod block terminals $\varphi_{dR}(z,s = 1)$ and one of the ends of rod homopolymer $\varphi_{hR}(z,s = 1 - f_{dC})$ in part b, for monolayer smectic-A (mA) with $f_{hR} = 0.1$ and bilayer smectic-A phases (bA) with $f_{hR} = 0.3$. $z = 0$ is located at the center of rod-rich area. The dashed line in part b denotes the rod block terminal distribution $\varphi_{dR}(z,s = 1)$ in pure rod−coil diblocks.

In particular, another distinction in Figure 4b is the appearance of a bilayer smectic-A (bA) phase in the weakly segregated area (χN = 6−8) when blended with a moderate amount of rod homopolymers. This is different from the prediction of Semenov[17] and Matsen et al.,[19] where the bA phase was observed at extremely large χN and small f_C with the assumption of completely rigid rod model. In our work, the wormlike chain model allows the rod blocks and homopolymers to have some degrees of chain bending fluctuation and disalignment along the nematic director, which can provide more interfacial area per coil block. With the increasing of μN (χN), the rods tend to orient better along the nematic director, resulting in the decrease of interfacial area per coil block. In order to increase the interfacial area for the requirement of coil stretching entropy, the rods interdigitate with each other leading to the transformation from the bA to mA. This result is quite similar to the phase behavior of the pure rod−coil diblocks originating from different geometrical asymmetry between rods and coils ($\beta = 2$) predicted in our previous work.[23] Therefore, the theoretical results suggest that the bA structure can be conveniently obtained by adding molecular weight matched rod homopolymers instead of synthesizing specific rod−coil diblocks with small β. In fact, both the addition of molecular weight matched rod homopolymers and decreasing β can efficiently increase the occupied interfacial area per coil block and control the competition between interfacial energy and stretching entropy of coil blocks, resulting in different smectic microstructures. To our knowledge, the microstructure change in the rod subdomains resulting from the rod homopolymer addition, i.e., the mA to bA transition, has not been reported in previous experimental and theoretical studies. To shed light on the solubilization mechanism of rod homopolymers and its effect on the stability of different smectic microstructures, we perform an investigation on the microstructure, including rod orientation and rod segment arrangement, as well as the lamellae period and rod−coil interfacial property.

Microstructure and Lamellae Period. According to the SCFT results, Figure 5 as an example shows the density distributions of the rod homopolymers $\varphi_{hR}(z)$, the coil blocks $\varphi_{dC}(z)$ and the rod blocks $\varphi_{dR}(z)$, as well as the terminals of the rod block $\varphi_{dR}(z,s = 1)$ and one of the chain ends in the rod homopolymers $\varphi_{hR}(z,s = 1 - f_{dC})$, as a function of f_{hR} for a rod−coil/rod blend under relatively weak segregation strength, χN = 8. Different from the rod blocks, the other terminal distribution $\varphi_{hR}(z,s = 0)$ equals to $\varphi_{hR}(z,s = 1 - f_{dC})$ because there are two same free ends in a rod homopolymer chain, and thus only $\varphi_{hR}(z,s = 1 - f_{dC})$ is chosen for discussion here. The corresponding microdomain sizes and their dependence on the volume fractions of rod homopolymers f_{hR} are summarized in Figure 6a. At relatively low volume fraction of the added rod homopolymers such as f_{hR} = 0.1 corresponding to f_C = 0.45, where the mA structure is found for pure rod−coil diblocks shown in Figure 4a, the rod blocks still uniformly distribute in the rod domain as depicted by $\varphi_{dR}(z)$ in

dx.doi.org/10.1021/jp201972n |J. Phys. Chem. B 2011, 115, 8390–8400

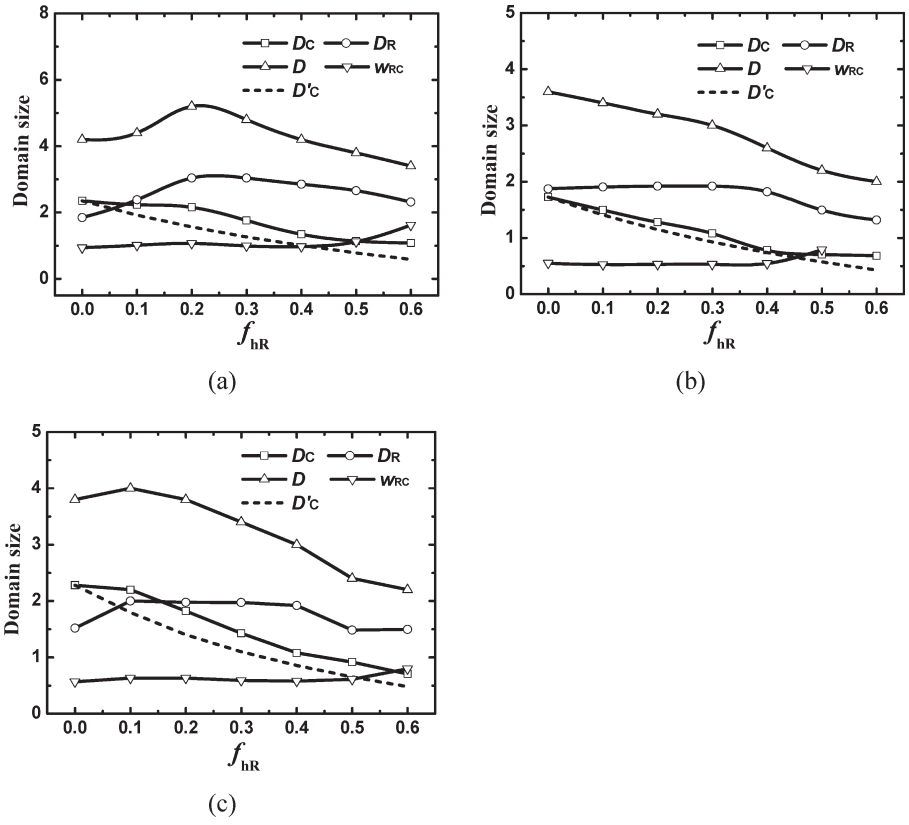

Figure 6. Domain sizes and lamellae period for a symmetric rod−coil diblock copolymer (f_{dC} = 0.5) blended with rod homopolymers as a function of f_{hR}, for two phase segregation strengths: (a) χN = 8, (b) χN = 12, and (c) asymmetric rod−coil diblock copolymer (f_{dC} = 0.6) blended with rod homopolymers under χN = 12. The dashed lines denote the scaling theory results for coil domain size D'_C, compared with SCFT.

Figure 5a. As shown by the density of rod block terminals in Figure 5b, the two-peak distribution of $\varphi_{dR}(z,s = 1)$ near the interface becomes weaker than the case of pure rod−coil diblocks due to the decrease of interdigitation in rod blocks, depicted by the shorter distance between two peaks of $\varphi_{dR}(z,s = 1)$. This results in a slight increase of D_R in Figure 6a as f_{hR} increase from 0 to 0.3. In addition, the small amount of added rod homopolymers mainly interdigitate into the smectic monolayer of rod blocks according to the density profile $\varphi_{hR}(z)$ in Figure 5a. The two density peaks of $\varphi_{hR}(z,s = 1 - f_{dC})$ in Figure 5b is similar to the rod block terminals $\varphi_{dR}(z,s = 1)$ in pure rod−coil diblocks. The addition of the homopolymers in the rod layer further increases the rod−coil laterally interfacial width, thus providing additional interfacial area for the coil blocks. In this case, the rod homopolymers and blocks rearrange to form a bilayer structure to decrease the interfacial energy. Taking f_{hR} = 0.3 as an example, the rod block density $\varphi_{dR}(z)$ starts to separate into two symmetric distributions in Figure 5a and the corresponding rod block terminal distribution, $\varphi_{dR}(z,s = 1)$ adopts one-peak at the center of rod-rich area in Figure 5b, suggesting the end-to-end arrangement of rods to form a bA structure. However the pure rod−coil block copolymers with the same coil volume fraction, i.e., f_C = 0.35, still adopt the mA structure in Figure 4a. During the transformation from the mA to bA structure in rod−coil/rod blends, the lamellae period D and rod domain size D_R all increase with f_{hR} as shown in Figure 6a. The rod homopolymers still keep the density distribution $\varphi_{hR}(z)$ within the rod domain in Figure 5a. In particular, $\varphi_{hR}(z,s = 1 - f_{dC})$ exhibits one primary peak in the middle of rod domain, suggesting the end-to-end arrangement of one free end, and two secondary peaks near the interface, which is the location of the other free end. As a result, a threshold for the lamellae period D and D_R occurs in Figure 6a, where both D and D_R reach the maximum values as the increasing of f_{hR}. After that D_R decreases due to the orientational disalignment of large amount of added rod homopolymers from the nematic direction **n**, i.e., the lamellae normal in the bA structure. This phenomenon has not been discussed in previous theoretic studies using completely rigid rod model, and difficult to be examined in experiment.[27] In contrast, the coil domain size D_C experiences a continuous decrease due to the less chain stretching of coil blocks along the increased laterally interfacial area, as a result of the interdigitation of rod homopolymers into the rod blocks. Therefore, the overall D decreases more obviously, as a result of the shrinkage both in D_R and D_C. However, the rod−coil interfacial width w_{RC} remains approximately unchanged because rod homopolymers do not penetrate into the coil domain and keep the liquid crystalline rod in the nanodomain structure due to the strong rod−rod interaction regardless of the amount of added rod homopolymers. In contrast the interfacial width w_{RC} in rod−coil/coil blends experiences a continuous increase with the penetration of coil homopolymers under the same interaction condition, i.e., χN = 8 and μN = 32 as discussed in Figure 3d.

When the phase segregation strength is increased, such as χN = 12 shown in Figure 6b, the mA−bA transition occurring at χN = 8 is never observed for the entire range of examined rod homopolymer fractions (f_{hR} = 0−0.6 corresponding to f_C = 0.5−0.2 in the phase diagram of Figure 4b). This is because the increased orientational interaction, i.e., μN = 48 induces a better

alignment of rods along the nematic direction. In this case, the rods pack more closely, thus decreasing the rod−rod lateral spacing. Therefore, the mA configuration favors coil stretching entropy than the bA. In particular, in the range of f_{hR} = 0−0.4 corresponding to f_C = 0.5−0.3, the microstructure of rod subdomains remains almost unchanged, exhibiting monolayer packing with well interdigitation between the rod homopolymers and blocks. As a result, the rod−coil interface is sharp and w_{RC} remains almost constant. While the coil blocks rearrange to occupy more laterally interfacial area, leading to a monotonic decrease of D_C and accordingly the decrease of D. This prediction is in agreement with experimental and other theoretical results.[27]

Similar to the discussion in section A, the coil domain size is also calculated as $D'_C = (D_{0,C})/(1 + X)$ according to the scaling theory,[27] where $D_{0,C}$ is the coil domain size of the pure rod−coil diblocks and X is the volume fraction ratio of the rod homopolymer to rod block component as $X = (f_{hR})/((1 - f_{hR})(1 - f_{dC}))$. This scaling theory is applicable in the strong segregation limit where the microstructure of rod nanodomains keeps unchanged and the interface broadening is not considered. In Figure 6a, the scaling theory overpredicts the decrease in coil domain size when the phase segregation is not so strong, i.e., χN = 8. This can be understood by the rearrangement of rods during the mA−bA transition, where the laterally interfacial area per coil block is smaller in the bA predicted by SCFT than that in the mA assumed by the scaling theory. The experimental study by Tao[27] et al. also found the departure from the scaling calculation. However, when the phase segregation is increased to χN = 12, as shown in Figure 6b, the SCFT results achieve a good agreement with the scaling argument for f_{hR} = 0−0.4. With further increasing of f_{hC}, the rod homopolymers are significantly separated from the interdigitated monolayer structure of rod blocks due to the increased translational entropy effects of free rod chains, which promotes a transition from mA to nematic phase. In this case, the rod−coil interfacial width w_{RC} experiences an obvious expansion, and the coil domain size D_C begins to depart from the scaling theory D'_C.

To further explore the effect of the added rod homopolymers on the smectic-C phase of pure rod−coil diblocks, a rod−coil diblock with f_{dC} = 0.6 at χN = 12 exhibiting mC structure is chosen to be blended with the molecular weight matched rod homopolymers in Figure 6c. In contrast to Figure 6b, the obvious feature in Figure 6c is the slight increase of D_R and D at small amount of homopolymer additions f_{hR} = 0−0.1. In this case, the tilt angle of rods to the lamellae normal in the mC structure decreases from 40° to 20° until a mA structure is formed at f_{hR} = 0.2. This decrease in the tilt angle of mC has also been observed experimentally in a blend system of rod−coil−rod triblock copolymers and rod homopolymers.[28] The mA structure for a range of f_{hR} = 0.2−0.6 remains unchanged with almost constant rod−coil interfacial width w_{RC}, similar to the case of rod−coil (f_{dC} = 0.5)/rod blends in Figure 6b. The resultant constant difference in D_C between SCFT and scaling theory results from the mA−mC transition predicted in SCFT, where the laterally interfacial area per coil block in the mC is larger than that in the mA due to the tilting angle between the nematic director **n** of rods and the lamellae normal.

CONCLUSIONS

The addition of coil or rod homopolymers on the phase behavior of rod−coil diblock copolymers is investigated systematically using a hybrid numerical SCFT method, in which the coils are modeled as Gaussian chains and the rods are modeled as wormlike chains. To simplify the presentation of the complicated parameter space, the ratio between microphase separation interaction and orientational interaction is characterized by a fixed ratio μ/χ = 4, and the size asymmetry between rods and coils is set as β = 4. In general, both the coil and rod homopolymers can enhance the stability of ordered phases according to the constructed phase diagram.

In the rod−coil/coil blends, the incorporation of the coil homopolymers expands the domain size of the swollen coil-rich area, which accounts for the monotonic increase in lamellae period. In particular, the ratio between the molecular weights of the homopolymers and the diblocks (α) plays an important role in the microstructure morphologies, including the subdomain sizes and interfacial width. For small molecular weight homopolymers, such as α = 1/8, 1/2, a good solubilization between coil homopolymers and their corresponding block domains is observed due to the mixing entropy effect of short homopolymer chains. In this case, the increase of coil domain size is not so obvious. As enhancing α, the stability of ordered smectic structures increases and the region of mC structure expands obviously in the phase diagram. A good agreement between SCFT and scaling theory is obtained when the blending coil homopolymers are of high enough molecular weight such as α = 1. In particular, the rod domain configuration and smectic interfacial property remain almost unchanged during the adding of different coil homopolymers, due to the dominant chain rigidity and liquid crystalline behavior of rods.

In the rod−coil/rod blends, the molecular weight matched rod homopolymers mainly interdigitate with the rod blocks in their sublayers, which will lose less entropy when approaching the wall and interface than coil chains. This effect plays an important role in stabilizing the smectic interfacial property, and significantly influences the microstructures. A mA−bA transition is predicted as the increase of homopolymer fraction under the weakly segregation region, which is similar to the phase behavior of pure rod−coil diblocks with a smaller size asymmetry parameter, i.e., β = 2 in our previous work. This implies that the bA structure can be obtained by conveniently blending molecular weight matched rod homopolymers into rod−coil diblocks, instead of synthesizing the rod−coil block copolymer with small size asymmetry between rod and coil (β). When the microphase separation increases to a strong segregation condition, i.e., χN = 12, the mA structure maintains unchanged and the SCFT results achieve a good agreement with the scaling theory. However for a mC configuration of the pure rod−coil diblocks, the rod homopolymer interdigitation will lead to a phase transition from the mC to mA, which is first observed in rod−coil/rod blends. As far as we know the current work is the first time to use the semiflexible chain SCFT to explore the self-assembled phase behavior of rod−coil diblock copolymer with homopolymer blends. The SCFT studies show that blending coil and rod homopolymers in the self-assembly of rod−coil block copolymers offers new insight into the fine control of microdomain sizes and stabilization of smectic microstructure for optimizing the organic optoelectronic device performance.

AUTHOR INFORMATION

Corresponding Author

*E-mail: pingtang@fudan.edu.cn.

■ ACKNOWLEDGMENT

We thank financial support from the National Basic Research Program of China (Grant Nos. 2008AA032101 and 2011CB6-05700) and funding from the NSF of China (Grant Nos. 20990-231 and 20874020) is also acknowledged.

■ REFERENCES

(1) Olsen, B. D.; Segalman, R. A. *Mater. Sci. Eng. R-Rep.* **2008**, *62* (2), 37–66.
(2) Segalman, R. A.; McCulloch, B.; Kirmayer, S.; Urban, J. J. *Macromolecules* **2009**, *42* (23), 9205–9216.
(3) Tao, Y. F.; Ma, B. W.; Segalman, R. A. *Macromolecules* **2008**, *41* (19), 7152–7159.
(4) Tao, Y. F.; McCulloch, B.; Kim, S.; Segalman, R. A. *Soft Matter* **2009**, *5* (21), 4219–4230.
(5) de Cuendias, A.; Hiorns, R. C.; Cloutet, E.; Vignau, L.; Cramail, H. *Polym. Int.* **2010**, *59* (11), 1452–1476.
(6) Sary, N.; Richard, F.; Brochon, C.; Leclerc, N.; Leveque, P.; Audinot, J. N.; Berson, S.; Heiser, T.; Hadziioannou, G.; Mezzenga, R. *Adv. Mater.* **2010**, *22* (6), 763–768.
(7) Chen, J. T.; Thomas, E. L.; Ober, C. K.; Mao, G. P. *Science* **1996**, *273* (5273), 343–346.
(8) Losik, M.; Kubowicz, S.; Smarsly, B.; Schlaad, H. *Eur. Phys. J. E* **2004**, *15* (4), 407–411.
(9) Chen, J. T.; Thomas, E. L.; Ober, C. K.; Hwang, S. S. *Macromolecules* **1995**, *28* (5), 1688–1697.
(10) Olsen, B. D.; Toney, M. F.; Segalman, R. A. *Langmuir* **2008**, *24* (5), 1604–1607.
(11) Tenneti, K. K.; Chen, X. F.; Li, C. Y.; Tu, Y. F.; Wan, X. H.; Zhou, Q. F.; Sics, I.; Hsiao, B. S. *J. Am. Chem. Soc.* **2005**, *127* (44), 15481–15490.
(12) Sary, N.; Rubatat, L.; Brochon, C.; Hadziioannou, G.; Ruokolainen, J.; Mezzenga, R. *Macromolecules* **2007**, *40* (19), 6990–6997.
(13) Olsen, B. D.; Segalman, R. A. *Macromolecules* **2005**, *38* (24), 10127–10137.
(14) Olsen, B. D.; Segalman, R. A. *Macromolecules* **2006**, *39* (20), 7078–7083.
(15) Olsen, B. D.; Shah, M.; Ganesan, V.; Segalman, R. A. *Macromolecules* **2008**, *41* (18), 6809–6817.
(16) Olsen, B. D.; Segalman, R. A. *Macromolecules* **2007**, *40* (19), 6922–6929.
(17) Semenov, A. N. *Mol. Cryst. Liq. Cryst.* **1991**, *209*, 191–199.
(18) Reenders, M.; ten Brinke, G. *Macromolecules* **2002**, *35* (8), 3266–3280.
(19) Matsen, M. W.; Barrett, C. *J. Chem. Phys.* **1998**, *109* (10), 4108–4118.
(20) Pryamitsyn, V.; Ganesan, V. *J. Chem. Phys.* **2004**, *120* (12), 5824–5838.
(21) Duchs, D.; Sullivan, D. E. *J. Phys.: Condens. Matter* **2002**, *14* (46), 12189–12202.
(22) Song, W. D.; Tang, P.; Zhang, H. D.; Yang, Y. L.; Shi, A. C. *Macromolecules* **2009**, *42* (16), 6300–6309.
(23) Song, W. D.; Tang, P.; Qiu, F.; Yang, Y. L.; Shi, A. C. *Soft Matter* **2011**, *7* (3), 929–938.
(24) Anthamatten, M.; Hammond, P. T. *J. Polym. Sci., Part B: Polym. Phys.* **2001**, *39* (21), 2671–2691.
(25) Shah, M.; Pryarnitsyn, V.; Ganesan, V. *Macromolecules* **2008**, *41* (1), 218–229.
(26) Potemkin, I. I.; Bodrova, A. S. *Macromolecules* **2009**, *42* (7), 2817–2825.
(27) Tao, Y. F.; Olsen, B. D.; Ganesan, V.; Segalman, R. A. *Macromolecules* **2007**, *40* (9), 3320–3327.
(28) Gao, L. C.; Yao, J. H.; Shen, Z.; Wu, Y. X.; Chen, X. F.; Fan, X. H.; Zhou, Q. F. *Macromolecules* **2009**, *42* (4), 1047–1050.
(29) Sary, N.; Mezzenga, R.; Brochon, C.; Hadziioannou, G.; Ruokolainen, J. *Macromolecules* **2007**, *40* (9), 3277–3286.
(30) Torikai, N.; Takabayashi, N.; Noda, I.; Koizumi, S.; Morii, Y.; Matsushita, Y. *Macromolecules* **1997**, *30* (19), 5698–5703.
(31) Matsen, M. W. *Macromolecules* **1995**, *28* (17), 5765–5773.
(32) Klymko, T.; Subbotin, A.; ten Brinke, G. *Macromolecules* **2007**, *40* (8), 2863–2871.
(33) Tamai, Y.; Sekine, R.; Aoki, H.; Ito, S. *Macromolecules* **2009**, *42* (12), 4224–4229.
(34) Vavasour, J. D.; Whitmore, M. D. *Macromolecules* **2001**, *34* (10), 3471–3483.
(35) Matsen, M. W. *J. Chem. Phys.* **1996**, *104* (19), 7758–7764.
(36) Matsen, M. W.; Schick, M. *Phys. Rev. Lett.* **1994**, *72* (16), 2660–2663.